Numerical simulation of the weld pool dynamics during pulsed laser welding using adapted heat source models

Article · September 2018

DOI: 10.1016/j.procir.2018.08.044

5 authors, including:

Fritz Lange
Fraunhofer Institution for Additive Production Technology IAPT
2 PUBLICATIONS **0** CITATIONS
SEE PROFILE

Antoni Artinov
Bundesanstalt für Materialforschung und -prüfung
13 PUBLICATIONS **2** CITATIONS
SEE PROFILE

Marcel Bachmann
Bundesanstalt für Materialforschung und -prüfung
39 PUBLICATIONS **241** CITATIONS
SEE PROFILE

Michael Rethmeier
Bundesanstalt für Materialforschung und -prüfung
224 PUBLICATIONS **1,575** CITATIONS
SEE PROFILE

Available online at www.sciencedirect.com

ScienceDirect

Procedia CIRP 74 (2018) 679–682

www.elsevier.com/locate/procedia

10th CIRP Conference on Photonic Technologies [LANE 2018]

Numerical simulation of the weld pool dynamics during pulsed laser welding using adapted heat source models

Fritz Lange[a], Antoni Artinov[a,]*, Marcel Bachmann[a], Michael Rethmeier[a,b], Kai Hilgenberg[a,b]

[a]*Federal Institute for Material Research and Testing, Unter den Eichen 87, 12205 Berlin, Germany*
[b]*Technical University Berlin, Straße des 17. Juni, 10623 Berlin, Germany*

* Corresponding author. Tel.: +49 3081043101. *E-mail address:* Antoni.Artinov@bam.de

Abstract

A transient simulation including the impact of the laser energy, the melting of the metal and the development of the weld pool was conducted to observe the evolution of the vapor capillary and the solidification of the melt in pulsed laser beam welding of AISI 304 steel. The phase field method was implemented to investigate the evolution and behavior of the liquid-gas interface during welding and to describe the condensed and vapor phases. The effects of phase transition, recoil pressure, thermo-capillary and natural convection, vaporization and temperature dependent material properties were taken into account. A Gaussian-like heat source under consideration of the Fresnel absorption model was used to model the energy input of the laser beam. The heat source model was extended by a newly developed empirical approach of describing multiple beam reflections in the keyhole. To validate this new model, the numerical results were compared to experimental data and good agreement regarding the size and shape of the weld pool was observed.

Peer-review under responsibility of the Bayerisches Laserzentrum GmbH.

Keywords: pulsed laser beam welding; weld pool dynamics; multiple reflections; vaporization

1. Introduction

Pulsed laser beam welding is a joining process especially valuable in the field of heat sensitive components. Heat affected zones can be kept small and thermal warping can be prevented due to cooling phases between single laser pulses. Hermetic seals, similar to weld seams of continuous wave mode lasers, can be achieved by producing overlapping pulse spots. Particularly in the area of heat sensitive, small measured devices, such as pacemakers, sensors or batteries, the prediction of the exact weld pool geometry is highly relevant [1]. Even comparatively low laser powers are sufficient in these applications.

Due to the complicated multi-physical phenomena that occur during practical welding the prediction of the weld pool shape is a complex problem. The in-situ experimental investigation of the weld pool is limited by high temperatures, strong illumination and expensive equipment [2] as well as its restriction to the weld pool surface. For this reason a numerical study is implemented to examine the development of the weld pool shape during the welding process. This approach needs to consider all relevant dynamics that take place in the molten metal and the influence of solidification during the cool down stage.

Furthermore experiments with an Yb: YAG-Laser are carried out to provide information about the accuracy of the simulation model. The simulation is designed in such a way that a direct comparison with cross-sections of the experimental weld spots is possible.

The energy input of a single laser pulse on a metal plate is examined for the simulative and experimental investigations. Comparable setups are implemented in literature for example in the works of Bruyere *et al.* [3]; [4], Courtois *et al.* [5] or Zhou *et al.* [6]; [7] with different assumptions and approaches regarding to physical phenomena and the description of multiple phases in the simulation domain. It has been shown

Peer-review under responsibility of the Bayerisches Laserzentrum GmbH.
10.1016/j.procir.2018.08.044

that the modelling of the heat source, as well as multiple reflections in the keyhole, have a non-negligible influence on the simulation results, compare with Chang *et al.* [8], Cho *et al.* [9], Lee *et al.* [10] and Ki *et al.* [11].

The aim of the present work is to develop an empirical model for a sufficiently accurate description of the additional energy input through multiple reflections of the laser beam in the keyhole. By this means an improvement of the accordance between numerical and experimental results is sought. This approach allows to use an empirical extension of the heat source model without implementing an additional modelling approach like the ray tracing method. In this way a simplification of the modelling process and a reduction of the calculation time can be achieved.

2. Mathematical Model

A two-dimensional, rotational symmetric and transient simulation is used to model the interaction of a single laser pulse of 300 W with a metal surface of standard AISI 304 steel. Therefore, a calculation domain with the geometric dimensions of 1.9 mm x 1.2 mm is set up. The commercial finite element software COMSOL Multiphysics 4.2 is used to solve the coupled equations of heat transfer and fluid flow.

A mesh of tetrahedral elements is used for the discretization of the simulation domain. The maximum element size in the domain is varying between 3.5×10^{-6} m in the area of heat transfer and the moving air-metal interface to 1×10^{-4} m in the heat affected zone depending on the influence of the physical processes at the numerical stability. Two areas are defined to indicate the initial position of the air-metal interface and the initial material distribution in the computational domain. The symmetry axis lies on the left border of the calculation domain, where also the center of the heat source is located. An outlet is defined on the upper boundary of the air region to enable a free fluid flow. No-slip conditions are set to the remaining boundaries to suppress velocities relative to the walls. Furthermore, adiabatic boundary conditions are defined for the heat transfer calculation, while the energy input is coupled with the phase field variable to limit it to the metallic phase of the simulation domain.

2.1. Assumptions

It is necessary to simplify the welding process in order to secure numerical stability and acceptable computing time. The basic assumptions made are:

- The fluid flow is laminar and incompressible.
- The material is isotropic and homogeneous.
- The Boussinesq approximation is used to model the free convection triggered by mass density changes due to its temperature dependence [12].
- The apparent heat capacity method is used to regard the latent heat of fusion [13].
- The shear stress on the keyhole wall triggered by leaking metal vapor is empirically determined, according to the approach of [14] and the kinetic theory of gases, remaining constant in the area of influence.
- The influence of surface active elements on the surface tension as well as the fluid flow and geometry of the weld pool is not considered, compare with [15].
- The influence of the metal vapor and the plasma in the keyhole on the total energy absorption of the workpiece is neglected. This is justifiable because the absorbed energy amount in the vapor is very small (especially for wavelengths around 1µm [16]) compared to the absorbed energy amount of the metal.

2.2. Governing equations

For the analysis of the fluid flow and heat transfer, solutions are found for the governing conservation equations of mass, energy and momentum.

The phase field method is used to model the two phases – air and metal – in the simulation domain and the behavior of the liquid-gas interface, as shown in [4]. The different aggregate states of the metal (solid and liquid) are taken into account by adapted material parameters and the approach of the modified viscosity, see [4]. Marangoni tension analogous to [17], recoil pressure considering the recondensation rate, compare with [18], [19] and Laplace forces, see [4], are considered at the liquid-gas interface. A smoothed representation of the interface between the phases is used to apply them as surface conditions, as shown by Bruyere *et al.* [4].

To take the shear stress on the liquid metal surface caused by the vapor flow into consideration, the order of its magnitude is found by the Darcy-Weisback equation, as shown by Métais *et al.* [14].

2.3. Heat source model

An immobile Gaussian heat source [8] is applied in the simulation while the Fresnel absorption model is used to depict the angle of incidence dependent changes in the absorption of laser beam energy on the metal surface [9], [20].

This approach leaves multiple reflections in the keyhole and their effect on the energy input into the material unconsidered. The most widely used attempt in literature to take them into consideration is the ray tracing method, see e.g. [9], [10] or [11]. Since many rays of the laser beam have to be calculated at each time step to get the exact distribution of laser energy on the surface, the computational effort is very high. For this reason an empirical model is developed to approximate the additionally introduced energy by multiple reflections in the keyhole.

In the case of a two-dimensional problem the reflected laser beam approximately produces a Gaussian-like energy distribution at the opposite keyhole wall. An increasing maximum angle of the keyhole wall will lead to an enhanced amount of energy reflected into the keyhole while the center of the additional heat source moves to the center of the keyhole.

This additional energy input Q is given by the following equation:

$$Q = F_A F_{Fresnel}\, q_1 \frac{2P}{\pi\left(R + (r_{max} - r_2)\right)} \cdot \exp\left(\frac{-\left(r - \left(M + \frac{r_2}{2}\right)\right)}{\frac{r_2^2}{2}}\right) \quad (1)$$

and is described by a Gaussian-like term that varies with the radial position r of the maximum surface angle α of the keyhole wall $M(r, \alpha)$. F_A is the amount of energy remaining after the first reflection of the laser beam at the keyhole wall. According to the Fresnel laws and the material dependent absorption coefficient, approximately 50 % to 60 % of the energy in this application is reflected during the first contact with the surface. The Fresnel absorption coefficient is taken into account by $F_{Fresnel}$. The laser power P and the effective radius R are analogous to the parameters of the conventional heat source model. r_{max} represents the maximum radius and r_2 the actual center position of the additional heat source depending on M. As a certain surface angle is needed to hit the opposite keyhole wall with a reflected beam, the parameter q_1 is used to disable the function below this angle.

3. Results

3.1. Experimental setup

The experiments are performed with an Yb: YAG-Laser with a wavelength of 1.07 µm. In accordance with the simulation model, the laser power is set to 300 W and the effective laser beam radius to 105 µm. The focal length amounts to 350 mm with the focal position set to the initial metal surface position. The laser beam is directed vertical to the metal surface. The welding process is executed with a standardized AISI 304 steel plate of 10 mm thickness. Temperature dependent material properties as well as phase change characteristics of this specific material are taken into account in the simulation. The surface of the metal is treated with face milling to reduce the influence of the surface roughness on the reflectivity and absorptivity properties of the surface and thus the resulting weld pool geometry. A welding scheme is used to minimize errors resulting from the manual grinding process during the preparation of cross-sections of the welding spots due to their very small dimensions. Therefore, the welding spots of each test series were arranged in a line with vertical offsets of 25 µm for each welding spot. In this way the error of manual grinding was limited to 0.5 % with respect to the geometry.

3.2. Numerical Results

First, the impact of the laser beam provides a rise of temperature in the metal and surrounding air. Subsequently, a weld pool develops as soon as melting temperature is reached.

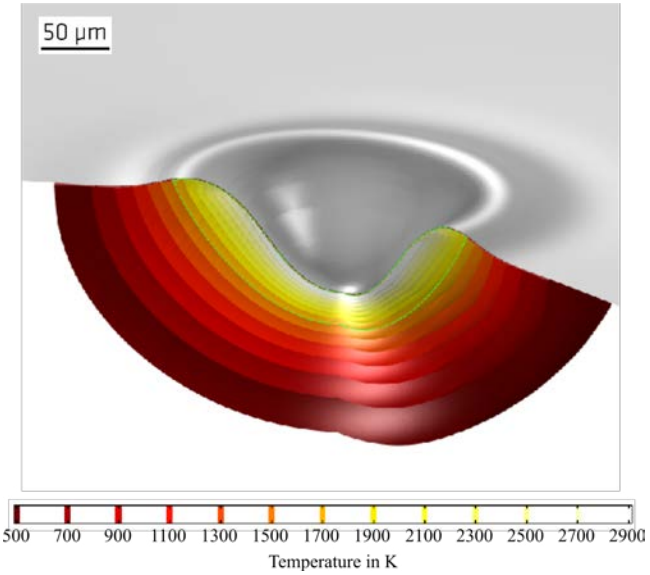

Fig. 1. Rotational extruded simulation results at 1.2 ms - the time of maximum elongation of the weld pool. The grey surface represents the metal-air surface found by evaluation of the phase field variable. Isothermal surfaces in the metal are shown, while the melt can be found between melting temperature of 1700 K and evaporation temperature of 3000 K.

The generation of a keyhole starts with achieving evaporation temperature at the surface. The deepening of the keyhole takes place along with the development of a bulge at the edge of the keyhole due to the influence of Marangoni effects and shear stress induced by metal vaporization. The energy input is shut down linearly after the laser peak plateau of 1 ms for reasons of numerical stability. Thus the energy input does not stop abruptly but decreases linearly over a period of another 1 ms. As a result the weld pool reaches its maximum elongation a few microseconds after the end of the laser peak stage, compare with Fig. 1. This has to be taken into account for the experimental investigation. During cooldown the closing of the keyhole can be observed while solidification of the weld pool takes place. At the final stage, the metal-air interface is nearly set back to the initial state.

The simulation result at 1.2 ms - the time of maximum elongation of the weld pool - is shown in Fig. 1. From this figure the geometry of the keyhole becomes apparent as well as the shape of the weld pool, which can be found between melting temperature (1700 K) and evaporation temperature (3000 K) of the examined steel.

The implementation of the additional term of multiple reflections to the heat source model, as described by equation (1), leads to enlarged weld pool geometries, as show in Fig. 2. The enlarged weld pool geometry can be traced back to the rise of total energy input in the course of the simulation. Special attention should be paid to the upper part of the weld pool shape. In this area the development of a nail-head shape can be observed that clearly agrees qualitatively with the experimental results whereas the conventional approach does not accomplish this detail, see Fig. 2. Furthermore the general accordance between the average experimental and the numerical results was improved by approximately 12.1 % with regard to the maximum width of the weld pool and approximately 10.5 % regarding to the maximum depth of the weld pool.

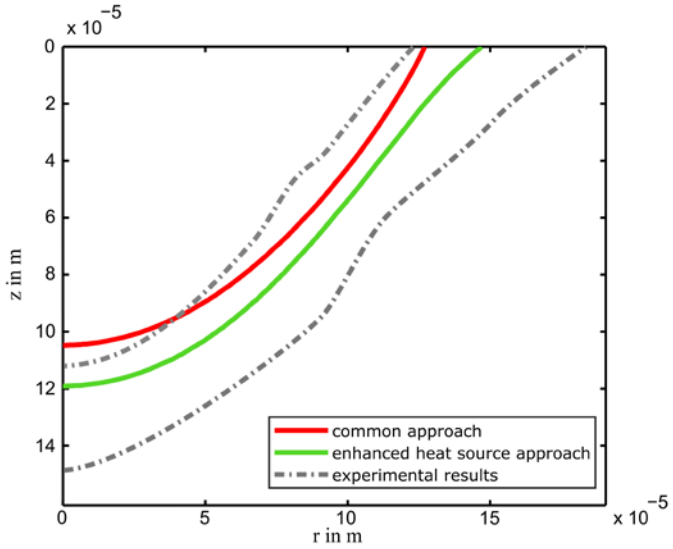

Fig. 2. Comparison between numerical and experimental results in the area from the symmetric axis and below the initial surface. The red line represents the simulation results for the common simulation approach under negligence of multiple reflections in the keyhole. The green line shows the weld pool geometry for the enhanced heat source model. The dot-dashed grey lines represent the minimum and maximum weld pool dimensions of the experimental results.

4. Conclusions

It can be concluded that an expansion of the heat source model by the empirical approach developed in this work increases the accordance between numerical and experimental results. These improvements do not only affect the geometric dimensions of the weld pool but also their shape. Especially the nail-head shape in the upper area of the weld pool complies much better with the experiments.

Nonetheless, slight differences between numerical and experimental results can still be noticed. These variations are mainly restricted to the dimensions of the weld pool, while the accordance of the qualitative shape itself could be clearly improved.

A possible explanation is that the introduced heat source model extension insufficiently describes further reflections of the laser beam in the keyhole. Especially the Fresnel absorption coefficient is calculated correctly only for the first reflection of the laser beam and assumed to be constant for additional reflections. This could be taken into consideration by further studies.

Acknowledgements

Financial funding of the Deutsche Forschungsgemeinschaft (DFG, German Research Foundation) under Grant No. BA 5555/1-1 is gratefully acknowledged.

References

[1] Kelkar G. Pulsed laser welding. WJM Technologies, Cerritos; 2000.
[2] Cho WI, Na SJ, Thomy C, Vollertsen F. Numerical simulation of molten pool dynamics in high power disk laser welding. Journal of Materials Processing Technology 212, 2012; p. 262-275.
[3] Bruyere V, Touvrey C, Namy P. Comparison between Phase Field and ALE Methods to model the Keyhole Digging during Spot Laser Welding. Rotterdam: COMSOL Conference; 2013.
[4] Bruyere V, Touvrey C, Namy P. A phase field approach to model laser power control in spot laser welding. Cambridge: COMSOL Conference; 2014.
[5] Courtois M, Carin M, Le Masson P, Gaied S. A two-dimensional axially-symmetric model of keyhole and melt pool dynamics during spot laser welding. Revue de Métallurgie 110; 2013. p. 165-173.
[6] Zhou J, Tsai HL, Wang PC. Transport phenomena and keyhole dynamics during pulsed laser welding. Journal of heat transfer 128; 2006. p. 680-690.
[7] Zhou J, Tsai HL. Effects of electromagnetic force on melt flow and porosity prevention in pulsed laser keyhole welding. International Journal of Heat and Mass transfer 50; 2007. p. 2217-2235.
[8] Chang WS, Na SJ. A study on the prediction of the laser weld shape with varying heat source equations and the thermal distortion of a small structure in micro-joining. Journal of Materials Processing Technology 120; 2002. p. 208-214.
[9] Cho JH, Na SJ. Implementation of real-time multiple reflection and Fresnel absorption of laser beam in keyhole. Journal of Physics D: Applied Physics 39; 2006.
[10] Lee JY, Ko SH, Farson DF, Yoo CD. Mechanism of keyhole formation and stability in stationary laser welding. Journal of Physics D: Applied Physics 35; 2002. p. 1570-1576.
[11] Ki H, Mohanty PS, Mazunder J. Modeling of laser keyhole welding, Part I, mathematical modeling, numerical methodology, role of recoil pressure, multiple reflections, and free surface evolution. Metallurgical and Materials Transactions A 33; 2002. p. 1817-1830.
[12] Faber TE. Fluid dynamics for physicists. Cambridge University Press.
[13] Hashemi HT, Sliepcevich CM. A numerical method for solving twodimensional problems of heat conduction with change of phase. Chemical engineering progress symposium series 63; 1967. p.34-41.
[14] Métais A, Matteï S, Tomashchuck I, Cicala E Gaied S. Dissimilar steels laser welding: Experimental and numerical assessment of weld mixing. Journal of Laser Applications 29; 2017.
[15] Bachmann M., Avilov V., Gumenyuk A., Rethmeier M. Numerical simulation of full-penetration laser beam welding of thick aluminium plates with inductive support. Journal of Physics D: Applied Physics 45; 035201.
[16] Hügel H, Duasinger F. Fundamentals of laser induced processes. Landolt Börnstein VII/1C; 2004.
[17] Saldi ZS, Kidess A, Kenjereš S, Zhao C, Richardson IM, Kleijn CR. Effect of enhanced heat and mass transport and flow reversal during cool down on weld pool shapes in laser spot welding of steel. International Journal of Heat and Mass Transfer 66; 2013. p. 879-888.
[18] Knight CJ. Theoretical modeling of rapid surface vaporization with back pressure. AIII Journal 17; 1979.
[19] Hirano K, Fabbro R. Study on striation generation process during laser cutting of steel. Ph. D. thesis; 2012.
[20] Ducharme R, Williams K, Kapadia P, Dowden J, Steen B and Glowacki M. The laser welding of thin metal sheets: an integrated keyhole and weld pool model with supporting experiments. Journal of Physics D: Applied Physics 27; 1994. p. 1619-1627.